

國立交通大學

光電工程學系 顯示科技研究所

碩士論文

低溫多晶矽薄膜電晶體微觀變動行為之
通道寬度相關性之研究



**Study on the Channel Width Dependence on the
Micro-Variation Behaviors of LTPS TFTs**

研究生：趙育德 Yu-Te Chao

指導教授：戴亞翔教授 Dr. Ya-Hsiang Tai

中華民國九十六年六月

低溫多晶矽薄膜電晶體微觀變動行為之
通道寬度相關性之研究


**Study on the Channel Width Dependence on the
Micro-Variation Behaviors of LTPS TFTs**

研究生：趙育德

Student：Yu-Te Chao

指導教授：戴亞翔教授

Advisor：Ya-Hsiang Tai



國立交通大學
光電工程學系 顯示科技研究所
碩士論文

A Thesis

Submitted to Department of Photonics Display Institute
College of Electrical Engineering and Computer Science
National Chiao Tung University

In partial Fulfillment of the Requirements

for the Degree of

Master

In

Display

June 2007

Hsinchu, Taiwan, Republic of China

中華民國九十六年六月

低溫多晶矽薄膜電晶體微觀變動行為之 通道寬度相關性之研究

研究生：趙育德

指導教授：戴亞翔教授

國立交通大學

光電工程學系 顯示科技研究所

中文摘要

多晶矽薄膜電晶體(poly-Si TFTs)基於其優於非晶矽薄膜電晶體(amorphous silicon TFTs)的電流驅動能力，最近在液晶顯示器(AMLCD)及有機發光二極體(AMOLED)顯示器的周邊電路整合應用上皆備受矚目。

在本論文中，我們將對低溫多晶矽薄膜電晶體(low temperature poly-Si TFTs)的元件特性作一統計性的研究。首先，我們先著重於元件的變動特性的研究。我們將元件的特性變動區分為巨觀變動及微觀變動。我們利用一種被稱為枕木型的元件排列方式，並經由調整元件間距離統計其電性行為的變動差異，驗證出相鄰的低溫多晶矽薄膜電晶體的主要變動來源是來自其微觀變動。為了探討微觀變動所引起的非匹配特性，我們藉由分析元件間參數差值的標準差來做探討，發現叉合(Interdigitated)方法比傳統方法具有更優越的特性，其中位障電壓與遷移率差值的標準差與叉合數目呈現反比，特別是位障電壓。因此我們提出一個微觀變動性的模型來加以描述叉合法的效能。在這個我們所提出的模型對於實際

量測到的分布比較中，經過回歸分析所得之回歸變異係數(R square) 皆在 0.98 以上。此一結果代表我們所提出的微觀變動性的模型與實際的分布情況十分吻合，也反映出該模型的適用性。此外，我們也將個別針對單晶矽及非晶矽的微觀變動性行為先做探討與研究，並將這些個別的結果詳細比較之，結果發現元件特性越佳的，它的微觀變動量會越小。

更進一步的，將這個提出來的模型試著應用在評估實驗數據無法解釋的變動性與大、小通道寬度間的關係。從模擬結果顯示，我們可以預測大通道寬度的微觀變動量，但是通道寬度小的微觀變動量，我們卻無法對他做預測。

先前關於低溫多晶矽薄膜電晶體的研究中主要著重於元件特性的改良。關於元件特性變動及其影響的問題很少被討論。然而，在低溫多晶矽薄膜電晶體能被廣泛使用於平面顯示技術前，其元件變動特性必須做進一步的研究。



Study on the Channel Width Dependence on the Micro-Variation Behaviors of LTPS TFTs

Student : Yu-Te Chao

Advisor : Prof. Ya-Hsiang Tai

Department of Photonics & Display Institute
National Chiao Tung University, Hsinchu, Taiwan

Abstract

Low Temperature Polycrystalline Silicon (LTPS) thin film transistors (TFTs) have attracted much attention in the application on the integrated peripheral circuits of display electronics such as active matrix liquid crystal displays (AMLCDs) and active matrix organic light emitting diodes (AMOLEDs) due to its better current driving compared with a-Si (amorphous silicon) TFTs.

In this thesis, the variation characteristics of LTPS TFTs are statistically investigated. Firstly we aim at the nature of device variation. We classify the variation as macro variation and micro variation. We adopt the “crosstie” layout to banish macro variation from micro variation. By analyzing the variance of electrical behavior with respect to difference device interval, we confirm that the main source of variation for the neighboring devices comes from the micro variation. In order to investigate the mismatching effects that cause by the micro variation, to analyze the standard deviations of parameters' differences, it is found that the interdigitated method is indeed superior than the original. Besides, threshold voltage and mobility are inversely proportional to the interdigit's finger numbers, especially the threshold

voltage. Therefore, a model of the micro variation is proposed to predict the performance of the interdigitated method, and it is proper to describe the variation behaviors with different device distances, for which the R square (Coefficient of Determinations) are higher than 0.98, which has high accuracy with the real data, reflecting the validity of the model. Besides, we applied the interdigitated method to the other devices with different grain structures, like the single crystal silicon and the amorphous silicon devices, and found that the micro variations of devices decline while device performance gets better. Furthermore, the proposed model is desired to evaluate the quantitative relationships between the variation and channel width in the regions where experimental data are not applicable. It is possible to be used to evaluate the variation of the larger channel width devices, but may not be capable of predicting the smaller channel width ones.

Most papers about LTPS TFTs are focusing on the improvement of device performance. Few papers aim at the device variation and the corresponding influence. However, before LTPS TFTs can be widely used in flat panel displays, the variation of these devices in mass production must be well-controlled.

致謝

感謝，我的指導教授 戴亞翔博士，總是耐心的給予指導，並且提供了這麼一個良好的資源與環境讓我得以專心學習。

感謝，士哲學長、泓緯學長、彥甫學長、皓彥學長與一德學長，謝謝你們不厭其煩的解決我許多課業上的問題，適時的督促我讓我往前邁進。

感謝，實驗室的同學們，亞諭、偉倫、晉煒、振業、仕承、秀娟以及建名，和你們的相處是我兩年來最快樂的時光，一起走過一起奮鬥的足跡我永遠也不會忘記。

感謝，實驗室的學弟妹們，曉嫻、長龍、明憲、小黑、首席、翔帥、阿貴、竹砲煒，謝謝你們的主動與貼心，在課業上以及生活上給予我許多的幫助。

感謝，我的好朋友們，香檳、教官、格禎、柯霸、鈺涵、永欣、佳渝、以及秀華，感謝你們長久以來的扶持與關懷，在我需要幫助的時候你們從來都不曾缺席。

最後我要感謝我最親愛的爸爸、媽媽、老姊、小妹，如果我有一點點的貢獻與成長，都是來自你們真誠無私的愛與無可替代的存在。

育德 2007.06.12

Contents

Chinese Abstract	I
English Abstract	II
Acknowledgment	VII
Contents	VIII
Figure Captions	X
Table Lists	XIV
Chapter 1- Introduction	1
1-1 Overview of Low-Temperature Polycrystalline-Silicon Thin-Film Transistors (LTPS) Technology	1
1-2 Review of Mismatch Effects in LTPS TFTs	2
1-2-1 Device Variation	2
1-2-2 Differential Pair	3
1-2-3 Mismatch Issue	4
1-3 Thesis Outline	6
Chapter 2- Experiments	8
2-1 Introduction to Crosstie TFTs	8
2-2 Device Fabrication and Measurements	9
2-3 Parameter Extration	10
2-4 Statistical Analysis	12
2-4-1 Average and Standard Deviation	12
2-4-2 Inter-Quartile Range	13
Chapter 3. Mismatch Analysis Based on Measurement Data	14
3-1 The Distribution of the Device Parameter Mismatch	14

3-2	Scaling Effects on the Mismatch	15
3-3	Other Devices With Different Grain Structures	19
Chapter 4-	Mismatch Analysis Based on Simulation	21
4-1	Simulation Concept and Method	21
4-2	Simulation for the Profile of Mismatch With Different Ranges	22
4-3	Simulation for the Mismatch With Different Distributions	23
4-3-1	Mismatch of the Devices With Small Channel Width	23
4-3-2	Mismatch of the Devices With Large Channel Width	25
4-4	Summary	26
Chapter 5-	Conclusion	27
References	29
Tables	32
Figures	65

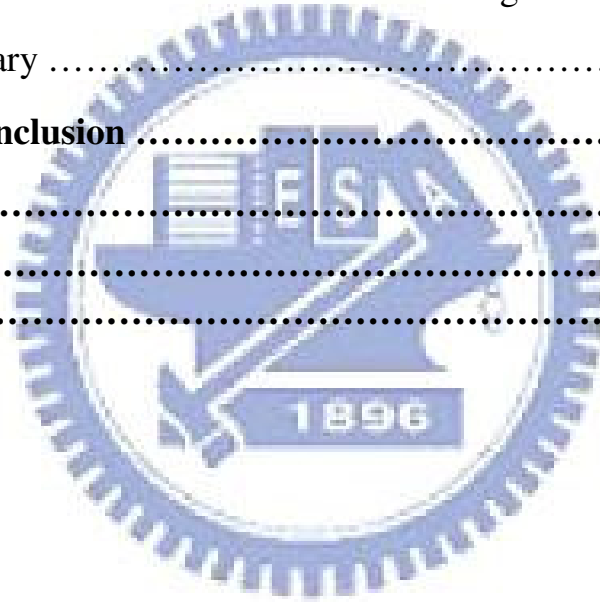


Figure captions

Chapter 1

Fig 1-1 The block diagram of an active matrix display.

Fig 1-2 The integration of peripheral circuits in a display achieved by poly-Si TFTs.

Fig 1-3 The purpose of matching is to have circuit performance based on the differential performance of two devices rather than the absolute performance of a single device.

Fig 1-4 Common-mode response in the presence of transistor mismatch (a) Differential pair sensing CM input. (b) equivalent circuit of (a).

Fig 1-5 The initial characteristics of LTPS TFTs are different from one another due to various distributions of grain boundaries.

Chapter 2

Fig 2-1 (a)The layout of the crosstie TFTs. (b) The distance of two nearest active regions is equally-spaced $40\mu\text{m}$.

Fig 2-2 The schematic cross-section structure of the n-type poly-Si TFT with lightly doped drain.

Fig 2-3 The schematic cross-section structure of the p-type poly-Si TFT without lightly doped drain.

Chapter 3

Fig 3-1-1 The threshold voltage distribution along the device position.

Fig 3-1-2 Simulation of the threshold voltage distribution along the device position for a long range.

Fig 3-1-3 The average and the standard deviation of the differences of threshold voltage of N-type devices(a)Poly-GroupA (b)Poly-GroupB.

Fig 3-1-4 The average and the standard deviation of the differences of mobility of N-type devices(a)Poly-GroupA (b)Poly-GroupB.

Fig 3-2-1 Illustration of the interdigitated method of the crosstie device.

Fig 3-2-2 Poly-GroupA N-type device distributions of threshold voltage difference between original and the interdigitated methods (a) interdigitated method of one-finger (b) interdigitated method of two-finger (c) interdigitated method of three-finger.

Fig 3-2-3 Poly-GroupA N-type device distributions of mobility difference between original and the interdigitated methods (a) interdigitated method of one-finger (b) interdigitated method of two-finger (c) interdigitated method of three-finger.

Fig 3-2-4 Poly-GroupA P-type device distributions of threshold voltage difference between original and the interdigitated methods (a) interdigitated method of one-finger (b) interdigitated method of two-finger (c) interdigitated method of three-finger.

Fig 3-2-5 Poly-GroupA P-type device distributions of mobility difference between original and the interdigitated methods (a) interdigitated method of one-finger (b) interdigitated method of two-finger (c) interdigitated method of three-finger.

Fig 3-2-6 Illustration of the interdigitated method of the crosstie device.

Fig 3-2-7 Measured data and model for devices with different channel width (a) \triangle

Vth of n-type device (b) ΔV_{th} of p-type device.

Fig 3-2-8 Measured data and model for devices with different channel width (a) Δ

Mu of n-type device (b) Δ Mu of p-type device.

Fig 3-3-1 The data of interdigitated method on ΔV_{th} of n-type for a-Si, poly-Si, and c-Si devices.

Fig 3-3-2 The data of interdigitated method on ΔV_{th} of p-type for a-Si, poly-Si, and c-Si devices.

Fig 3-3-3 The data of interdigitated method on Δ beta of n-type for a-Si, poly-Si, and c-Si devices.

Fig 3-3-4 The data of interdigitated method on Δ beta of p-type for a-Si, poly-Si, and c-Si devices.

Chapter 4

Fig. 4-1 This diagram shows the R square value on right vertical axis and standard deviation on left vertical axis for V_{th} mismatch of the experimental data. We classify this diagram into three regions, region I, region II and region III, by yellow dotted lines

Fig. 4-2 Simple distribution with four variables

Fig. 4-3 The chart for data transformation

Fig. 4-4 This diagram shows the selected row data and classifies it into two groups, Method A and Method B

Fig. 4-5 This diagram shows the Gaussian distribution with different ranges, $\gamma = 2$ and $\gamma = 4$, where parameter “ γ ” stands for the standard deviation.

Fig. 4-6 Use Gaussian distribution to simulate the different range for V_{th} mismatch. The black, red and green lines respectively represent the standard deviation

$\gamma = 1$, $\gamma = 3$ and $\gamma = 9$.

Fig. 4-7 Use Gaussian distribution to simulate the different range for Mu mismatch.

The black, red and green lines respectively represent the standard deviation

$\gamma = 1$, $\gamma = 3$ and $\gamma = 9$.

Fig. 4-8 (a)Gaussian distribution (b)Lorentzian distribution (c)Gauss-Lorentzian distribution (d)Uniform distribution

Fig. 4-9 The R square value on right vertical axis and the standard deviation on left vertical axis with respect to the device size for Vth of (a)Method A and (b)Method B

Fig. 4-10 The R square value on right vertical axis and the standard deviation on left vertical axis with respect to the device size for Mu of (a)Method A and (b)Method B

Fig. 4-11 The statistical diagram of the Uniform distribution for Method B with one-finger, five-finger, ten-finger and fifty-finger

Fig. 4-12 The data of (a) ΔV_{th} and (b) $\Delta \mu$ of one-finger to six-finger from the experiment and the simulation of Method A and Method B

Fig. 4-13 The Vth mismatch of sixty-four-finger for Method A with the fitting equations displayed inside the diagram

Fig. 4-14 The Mu mismatch of sixty-four-finger for Method A with the fitting equations displayed inside the diagram

Table Lists

Chapter 3

Table3-1 The standard deviation of ΔV_{th} and $\Delta \mu_{0}$ for n-type devices

Table3-2 The standard deviation of ΔV_{th} and $\Delta \mu_{0}$ for p-type devices

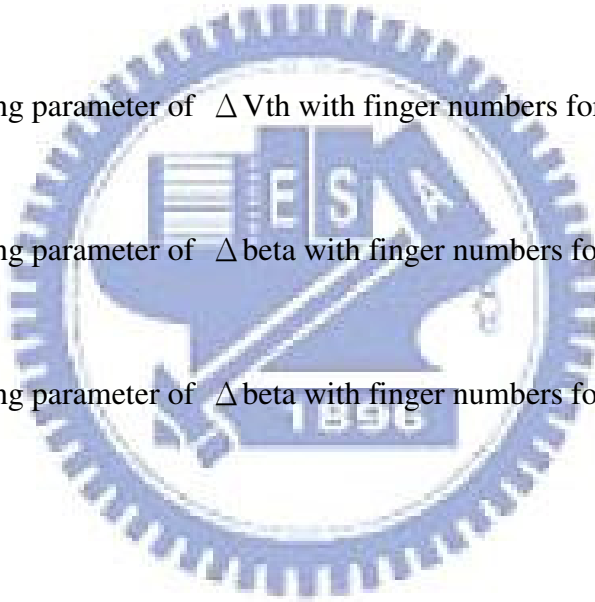
Table3-3 The fitting parameter of the proposed model for the Poly-GroupA and Poly-GroupB devices

Table3-4 The fitting parameter of ΔV_{th} with finger numbers for n-type different devices

Table3-5 The fitting parameter of ΔV_{th} with finger numbers for p-type different devices

Table3-6 The fitting parameter of $\Delta \beta$ with finger numbers for n-type different devices

Table3-7 The fitting parameter of $\Delta \beta$ with finger numbers for p-type different devices



Chapter 4

Table4-1 The fitting parameters of the V_{th} mismatch for the simulation of different range

Table4-2 The fitting parameters of the μ mismatch for the simulation of different range

Table4-3 The equations and the parameters for the different distributions

Table4-4 The R square values of the fitting parameters based on equation (3-1) and exponential laws for the experiment data, and Method A, and Method B